LANGMUIR

pubs.acs.org/Langmuir Article

Surface Nanodroplet-Based Extraction Combined with Offline Analytic Techniques for Chemical Detection and Quantification

Zhengxin Li, Hongyan Wu, Jae Bem You, Xiaomeng Wang, Hongbo Zeng, Detlef Lohse, and Xuehua Zhang*

Cite This: *Langmuir* 2022, 38, 11227−11235 Read Online

ACCESS | Metrics & More | Article Recommendations | Supporting Information

ABSTRACT: Liquid−liquid extraction based on surface nanodroplets can be a green and sustainable technique to extract and concentrate analytes from a sample flow. However, because of the extremely small volume of each droplet (<10 fL, tens of micrometers in base radius and a few or less than 1 μm in height), only a few in situ analytical techniques, such as surface-enhanced Raman spectroscopy, were applicable for the online detection and analysis based on nanodroplet extraction. To demonstrate the versatility of surface nanodroplet-based extraction, in this work, the formation of octanol surface nanodroplets and extraction were performed inside a 3 m Teflon capillary tube. After extraction, surface nanodroplets were collected by injecting air into the tube, by which the contact line of surface droplets was collected by the capillary force. As the capillary allows for the formation of $\sim 10^{12}$ surface nanodroplets on the capillary wall, ≥2 mL of octanol can be collected after extraction. The volume of the collected octanol was enough for the analysis of offline analytical techniques such as UV−vis, GC-MS, and others. Coupled with UV−vis, reliable extraction and detection of two common water pollutants, triclosan and chlorpyrifos, was shown by a linear relationship between the analyte concentration in the sample solution and UV−vis absorbance. Moreover, the limit of detection (LOD) as low as 2×10^{-9} M for triclosan (~0.58 μg/L) and 3×10^{-9} M for chlorpyrifos (~1.05 μg/L) could be achieved. The collected surface droplets were also analyzed via gas chromatography (GC) and fluorescence microscopy. Our work shows that surface nanodroplet extraction may potentially streamline the process in sample pretreatment for sensitive chemical detection and quantification by using common analytic tools.

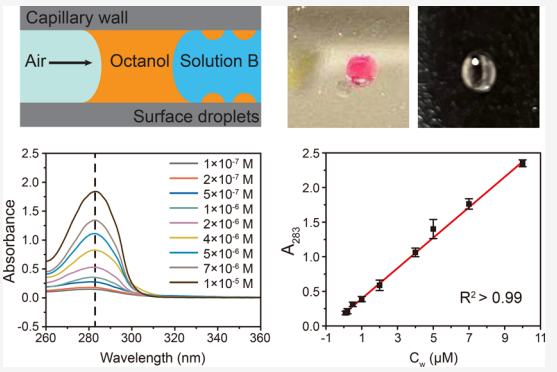

INTRODUCTION

Reliable detection and analysis of chemicals is crucial in many areas including water pollutant detection,[1,2] air quality monitoring,[3,4] analysis of drugs and pharmaceuticals,[5,6] biological sensing,[7,8] and food quality control.[9−11] To enhance the detection sensitivity, the compounds of interest are often preconcentrated by using an extractant material. Liquid−liquid microextraction has been widely used to achieve this purpose. In a liquid−liquid microextraction, a small volume of nonsoluble extractant droplet is exposed to the sample to selectively extract the target chemicals by chemical partitioning.[12] The high surface area-to-volume ratio of the extractant droplet allows efficient mass transfer across the droplet−sample interface.[13,14]

Among various liquid-phase microextraction processes,[15−18] dispersive liquid−liquid microextraction (DLLME) is one of the most widely used methods for sample preconcentration because of its simplicity and high extraction efficiency.[18,19] In a typical process of DLLME, emulsion droplets are spontaneously formed upon mixing of a water-immiscible extractant, a dispersive cosolvent, and an aqueous solution of the target analyte.[19] Because of the high partition coefficient of the extractant, target analytes are extracted from the aqueous phase to the extractant droplets. The droplets are separated and collected from the bulk phase and analyzed by sensitive analytical techniques such as gas chromatography−mass spectrometry (GC-MS),[11,20] high-performance liquid chromatography (HPLC),[21,22] ultraviolet−visible spectroscopy (UV−vis),[23] and atomic absorption spectrometry.[2] Despite the excellent extraction performance and simplicity, DLLME often uses environmentally harmful extractants such as chlorobenzene, chloroform, and carbon tetrachloride and consumes lots of dispersive solvents, such as ethanol and acetone.[19,24,25] Additionally, emulsion droplets need to be separated and collected from the bulk by using separation equipment.

Received: May 18, 2022
Revised: August 21, 2022
Published: September 6, 2022

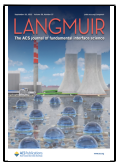

https://doi.org/10.1021/acs.langmuir.2c01242
Langmuir 2022, 38, 11227−11235

Surface nanodroplets serve as an effective platform to address several drawbacks of liquid−liquid extraction. Surface nanodroplets are femtoliter droplets formed on a solid surface by the solvent exchange method in which a ternary mixture of solvent, antisolvent, and oil (i.e., extractant) is replaced with fresh antisolvent. As the fresh antisolvent replaces the ternary mixture, the oil becomes oversaturated which leads to nucleation and growth of the surface nanodroplets on a target substrate.[26] The solvent exchange method enables controlled formation of the nanodroplets over a large area that has led to applications in various fields such as chemical reaction,[27,28] chemical analysis,[29] and optics, to name but a few.[30] Recently, the capability of surface nanodroplets to extract target analytes from various samples[31] was leveraged for the quantification of acids in beverages[28,32] as well as for the detection fluorescent compounds from dense suspensions.[33]

However, although the surface nanodroplets are highly efficient for extraction, the fact that they are pinned on a substrate and that the volume of each nanodroplet is on the femtoliter scale make the collection of these nanodroplets extremely challenging by conventional methods such as centrifugation. While in situ analytical techniques such as surface-enhanced Raman spectroscopy (SERS)[31] or optical microscopy[33] can be employed for analysis during extraction, a method to collect the droplets would greatly expand the applicability of surface nanodroplet-based extraction method as it would enable the use of offline analytical techniques such as GC-MS, HPLC, UV−vis, and others.

In this work, the formation of surface nanodroplets and droplet extraction were performed in a 3 m hydrophobic capillary tube. After extraction, enough surface nanodroplets (total volume ≥2 μL) were collected from the capillary and analyzed by UV−vis. The extraction performance was evaluated by using two common pollutants, e.g., triclosan and chlorpyrifos, and optimized by varying the total volume of the sample solution and for submilliliter samples. The process of droplet formation and extraction were sped up by increasing the sample flow rate. The flexibility of the method was also tested by coupling with GC and fluorescence microscopy. The approach reported in our work is environmentally friendly, as no harmful or toxic solvent is required and a limited quantity of solvents are needed during the entire process of droplet formation, nanoextraction, and droplet collection. Although the extraction in microfluidic devices is already known and studied extensively, the novelty of our method is stationary nanodroplets immobilized on the inner wall, which allows extraction of an analyte from a large volume of the sample solution and enables highly efficient extraction and enrichment.

METHODOLOGY

Chemicals and Materials. Ethanol (≥89%, Fisher Scientific) was used as the cosolvent for droplet formation. 1-Octanol (≥99%, Fisher Scientific) was selected as the droplet liquid/extractant. Triclosan (≥98%, TCI America), chlorpyrifos (AR, Sigma-Aldrich), and Nile red (≥99%, Acros Organics) were selected as the analytes for droplet extraction. All chemicals were used as received without any further purification. Water (18.2 MΩ·cm) was obtained from a Milli-Q purification unit (MilliporeSigma).

Droplet formation and extraction were performed in a 3 m Teflon capillary tube (MilliporeSigma) with an inner diameter (ID) of 0.8 mm and an outer diameter (OD) of 1.58 mm. Before use, water and ethanol were successively injected into the capillary tube for cleaning. After cleaning, the capillary tube was dried by injecting a stream of air.

Droplet Formation and Nanoextraction. Surface nanodroplets were produced on the inner wall of the Teflon capillary by the solvent exchange process. Figure 1A sketches the setup in which two shut-off valves and a T-junction were used to connect the tube and the syringe. The valves and T-junction were used to prevent trapping air and guarantee the mixing of two solutions. The solutions were injected into the tube with a constant flow rate by a syringe pump (New Era, NE-1000). When injecting solutions into the tube, only the valve to the tube was open. If the air was trapped during the exchange of the syringes, the valve to the tube was closed and the valve to the waste was opened to remove the air.

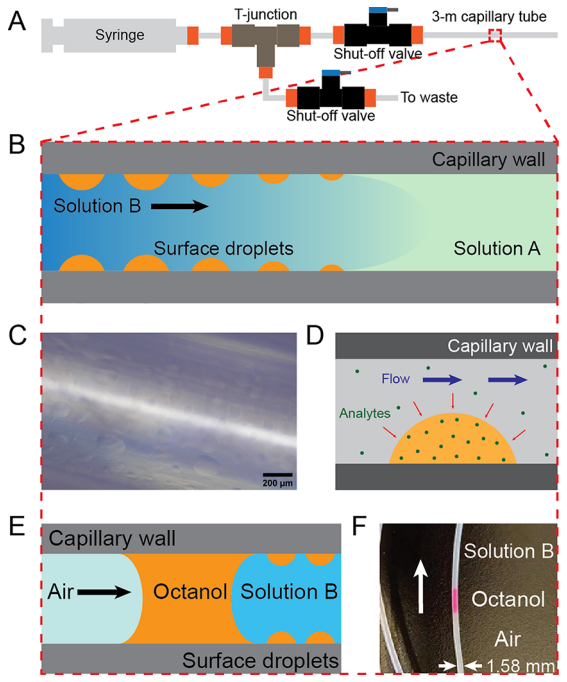

Figure 1. (A) Schematic of the experimental setup for droplet formation and extraction. (B) Schematic of the droplet formation on the inner wall of a Teflon capillary tube by the solvent exchange process. (C) An optical image of octanol droplets on the inner wall of a capillary tube. (D) A sketch showing the extraction process of analytes into a surface droplet by flowing the sample solution in the capillary tube. (E) Schematic of octanol collected by the capillary force between water and air. (F) Image of octanol collected in the capillary tube.

During the solvent exchange, a solution of the droplet liquid (solution A) in the capillary tube was displaced by a water sample with dissolved analytes (solution B) which should be a poor solvent for the droplet liquid. In our experiments, solution A was 3.5 vol % octanol in water/ethanol mixture (1:1, v/v). Solution B was the water sample with 0.04 vol % octanol and the dissolved analytes. For samples with chlorpyrifos as solution B, the solutions also contain 0.05 vol % ethanol. As sketched in Figure 1B, octanol surface nanodroplets nucleated out and grew on the inner wall of the capillary due to the solubility gap of octanol in solution A and solution B. Figure 1C demonstrates an optical image of octanol surface nanodroplets formed on the capillary wall (Nikon H600L, 4× objective lens).

https://doi.org/10.1021/acs.langmuir.2c01242
Langmuir 2022, 38, 11227−11235

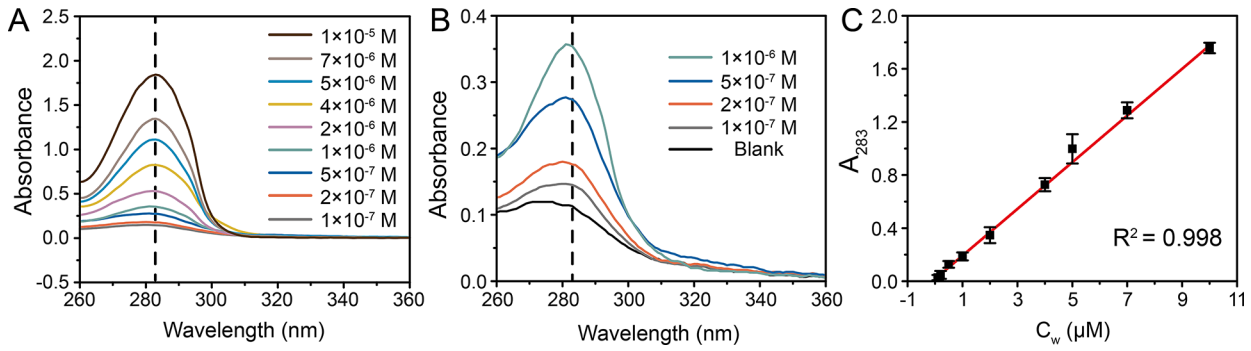

Figure 2. (A) UV−vis absorbance spectrum of collected octanol droplets. The droplets were from samples with analyte (triclosan) concentration C_w of 10^{-5}−5×10^{-8} M. The volume flow rate Q and the total volume of the sample solution V were 10 mL/h and 1.6 mL. (B) Zoom-in of UV−vis absorbance in (A). (C) Absorbance at 283 nm A_{283} as a function of C_w. The error bars (standard deviation) are from three replicates.

Figure 1D illustrates the extraction of analytes from solution B into the octanol surface nanodroplet, at the same time as droplet formation by the solvent exchange process was taking place. Because of the pinning effect of surface droplets on the capillary wall, the nanodroplets were stable and could not be removed by the flow of solution B. After injecting ∼1.6 mL of solution B into the tube, most of the ethanol was removed, and the solvent exchange was almost finished that droplets would not grow further. At this point, the injection of sample solution can be stopped or continued for further extraction.

Sample Collection and Instrumentation. After the extraction of analytes from the sample solution, air was slowly introduced into the capillary tube by the syringe pump. The flow rate of the air was kept at 5 mL/h. Because of the capillary force, octanol droplets with the extracted analytes can be collected between water (i.e., solution B) and air, as illustrated in Figure 1E. Figure 1F shows an image of collected octanol between air and water sample. With Nile red extracted from the water sample, the collected octanol appeared in red in the screenshot.

After all of the water sample was pushed out by air, ≥2 μL of the octanol sample containing the analytes could be collected for analysis. A microvolume ultraviolet−visible (UV−vis) spectrophotometer (Nanodrop 2000c, Thermo Fisher) was used for the detection of triclosan and chlorpyrifos. The UV−vis spectrum of octanol standards containing target analytes was used to establish a calibration curve from the Beer−Lambert law. The calibration curve was then used to determine the concentration of the target analyte in extractant droplets C_d. The limit of detection was roughly estimated by reducing analyte concentration C_w in controlled experiments. The existence of the analyte was confirmed by three replicates with positive absorbance compared with the blank group. The shifted contaminant peak, which is a result of the superposition of the absorbance from the background and analytes, was taken as another necessary feature to confirm the presence of analytes.

Instrumental analysis was also performed on a gas chromatograph/mass spectrometer (Agilent 6890 with 5975B MSD) for the octanol sample with triclosan. The procedure is based on a previously published method.[34] Briefly, a HP-5MS GC column was used for the separation. The GC/MS injector and the transfer line temperature were set to 280 and 300 °C, respectively. The temperature program was initiated with 75 °C for 1 min, increased to 230 °C at 10 °C, then to 280 °C at 20 °C/min, and held for 15 min. The droplet sample was diluted in dichloromethane (DCM), and the sample injection volume was 2 μL. The mobile phase is helium, and the flow rate is 1.2 mL/min. The presence of Nile red in octanol was determined by an optical microscope (Nikon H600L, 4× objective lens).

RESULTS AND DISCUSSION

Performance of Triclosan Extraction. As a commonly used antibacterial and antifungal agent,[35,36] triclosan in the water sample was taken as the model compound. The volume flow rate Q and total volume V of the sample solution were 10 mL/h and 1.6 mL.

The UV−vis absorbance spectrum of collected octanol nanodroplets after extraction of triclosan is shown in Figure 2A. The absorbance peak at 283 nm was found to increase with increasing triclosan concentration in the sample. This is consistent with the characteristic triclosan absorbance peak reported in the literature.[37] Figure 2B shows a zoomed-in view of the absorbance spectrum from samples with C_w below 10^{-6} M, plotted together with a blank group without triclosan in sample solution. C_w is the analyte concentration in the sample. The characteristic peak for triclosan is still detectable even from the sample with C_w of 10^{-7} M and can be easily distinguished from a wide background peak spanning between 270 and 280 nm present in the blank group. Overlap of the background peak and the characteristic peak at the C_w of 10^{-7} M leads to the highest absorbance appearing at 280 nm. C_w below 10^{-7} M leads to indistinguishable absorbance from the background and the analyte. The absorbance at 283 nm (A_{283}) is plotted as a function of C_w in Figure 2C. A linear relationship was found between C_w and A_{283}, as demonstrated by the fitting in Figure 2C. A_{283} contributed from the background was corrected by subtracting A_{283} in the blank group.

To quantify the concentration of triclosan in octanol nanodroplets (C_d), the UV−vis spectra of triclosan in octanol standard solutions were obtained as shown in Figure 3A. From the Beer−Lambert law, C_d and A_{283} are linearly correlated as shown in Figure 3B. With the linear relationship between C_d and A_{283}, C_d of collected octanol droplets in experiments can be calculated as a function of C_w, as shown in Figure 3C. The extraction method was further optimized by varying the sample flow rate and sample volume in the following sections.

The enrichment factor (EF) defined as C_d/C_w was calculated from Figure 3C and plotted as a function of C_w in Figure 3D. For the sample concentration C_w of 10^{-5}−5×10^{-6} M, the EF fluctuated in a small range from 350 to 430. As the volume of collected octanol was ∼3 μL for the extraction from the 1.6 mL sample, the recovery of triclosan was estimated to be between

https://doi.org/10.1021/acs.langmuir.2c01242
Langmuir 2022, 38, 11227−11235

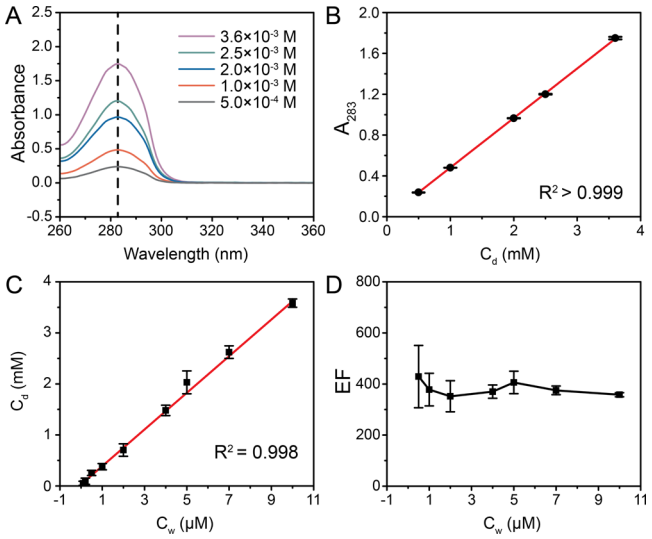

Figure 3. (A) UV−vis absorbance spectrum of triclosan in octanol standard solutions. The concentration of triclosan in octanol solutions are from 10^{-4} to 3.6×10^{-3} M. (B) A_{283} as a function of triclosan concentration in octanol droplets C_d. (C) C_d as a function of C_w. (D) Enrichment factor (EF) as a function of C_w.

66% and 77%, which could be because we only collected a portion of octanol droplets, not all the octanol droplets on the inner wall of the tube. At the same time, the standard deviation of EF calculated from three replicates also increased with the decrease of C_d. As the quantification of triclosan below 5×10^{-7} M may not be accurate, these data are not included in Figure 3D.

Effects from Volume Flow Rate *Q* on the Extraction. The high reproducibility of the nanodroplet extraction was confirmed at different flow rates of sample solution. A triclosan solution (4×10^{-6} M) with 1.6 mL of volume was used. The flow rate Q of the sample solution was varied from 10 to 50 mL/h. Figure 4A plots the UV−vis absorbance spectrum of the collected nanodroplets obtained by using various flow rates. The characteristic peak of triclosan at 283 nm remained similar as Q increased from 10 to 50 mL/h. As Figure 4B shows, A_{283} only slightly decreases with the increase of Q.

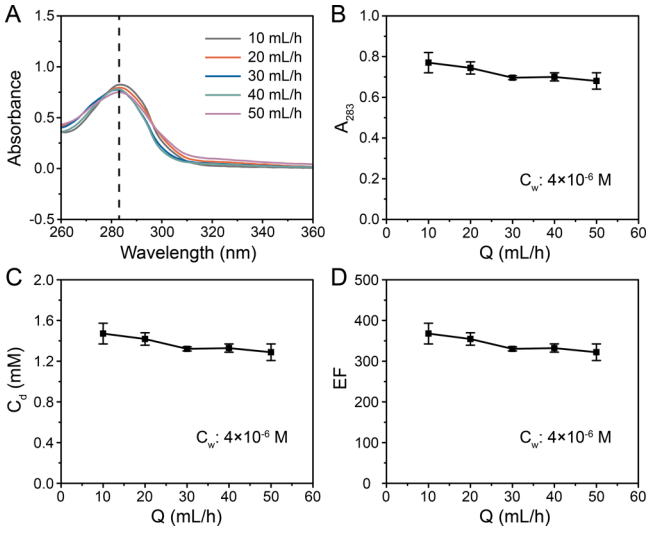

Figure 4. (A) UV−vis absorbance spectrum of collected octanol droplets. The droplets were from extractions with Q from 10 to 50 mL/h. C_w and V of the samples were 4×10^{-6} M and 1.6 mL. (B) A_{283} as a function of Q. (C) C_d as a function of C_w. (D) EF as a function of C_w.

From results of standard solutions in Figure 3A,B, C_d and EF were estimated and plotted as the functions of Q in Figure 4C,D. The influence from Q on extraction performance are found to be negligible. Thus, increasing Q can be an effective method to speed up the extraction process without much compromise of the extraction performance. Take the extraction from Q = 10 mL/h and Q = 50 mL/h, for instance, the time spent for nanodroplet formation and extraction was reduced from ∼10 to ∼2 min, while A_{283} and EF only decreased ∼13%.

The independence of enrichment factor on flow rate is related to the consistent droplet sizes in the capillary tube. In a previously published work, the size distribution of surface nanodroplets formed by the solvent exchange was also found to be irrelevant to the flow rate in the capillary.[33] This is in contrast to results on a flat substrate in a flow chamber, in which droplets tend to be larger at a higher flow rate.[26] The geometry confinement in the capillary blocks the effect from the external flow on the mass transfer of the surface droplets, which contributes to the trivial dependence of the extraction performance on the flow rate.[33]

Effects from Sample Volume *V* on the Extraction. The extraction performance was further studied by varying the sample volume (V). The sample flow rate (Q) and C_w were kept at 10 mL/h and 1×10^{-6} M. After the injection of 1.6 mL of triclosan sample solution, only water can be collected at the outlet. All ethanol was removed from the capillary, so that droplet formation stopped. The extraction performance was tested from samples with V up to 10 mL, in which extraction continued after droplet formation. A sample with V of 0.8 mL was also tested, in which the extraction was finished before all ethanol was removed from the capillary. The UV−vis spectrum of the collected droplets is plotted in Figure 5A, reflecting a higher peak with the increase of the sample volume V. Figure 5B shows A_{283} monotonically increases with V.

From results in Figure 5B, C_d and EF were calculated and plotted as the functions of C_w in Figure 5C,D. Increasing V clearly enhanced the extraction performance reflected by the increase in EF from ∼400 to ∼2400 when V increased from 1.6 to 10 mL. As only ∼2 μL of octanol was collected at V = 10 mL extraction, the recovery of triclosan was estimated to be ∼48%. Moreover, signals from a low sample volume of V = 0.8 mL suggest that the droplet extraction in the capillary can also be applied to submicroliter samples that are not sufficient to finish the solvent exchange. As EF calculated from our experiments is much smaller than the partition coefficient of triclosan between octanol and water (pK_{ow} = 4.76), C_d in droplets has not reached equilibrium with C_w in the sample solution even at the highest EF of 2400. Triclosan can be continuously extracted from the sample flow if higher volume is used.

We did not further increase the sample volume at the same triclosan concentration, as the micro-UV−vis spectrometer we used cannot detect very strong absorbance (>3). The absorbance of all our samples was below this upper limit. Instead, 100 mL samples with lower C_w were tested to further enhance the LOD of the method. As droplets slowly dissolved in the sample flow, we increased the octanol volume ratio in solution A to 4 vol % to produce larger octanol droplets. Our previous work has systematically investigated the influence of

https://doi.org/10.1021/acs.langmuir.2c01242
Langmuir 2022, 38, 11227−11235

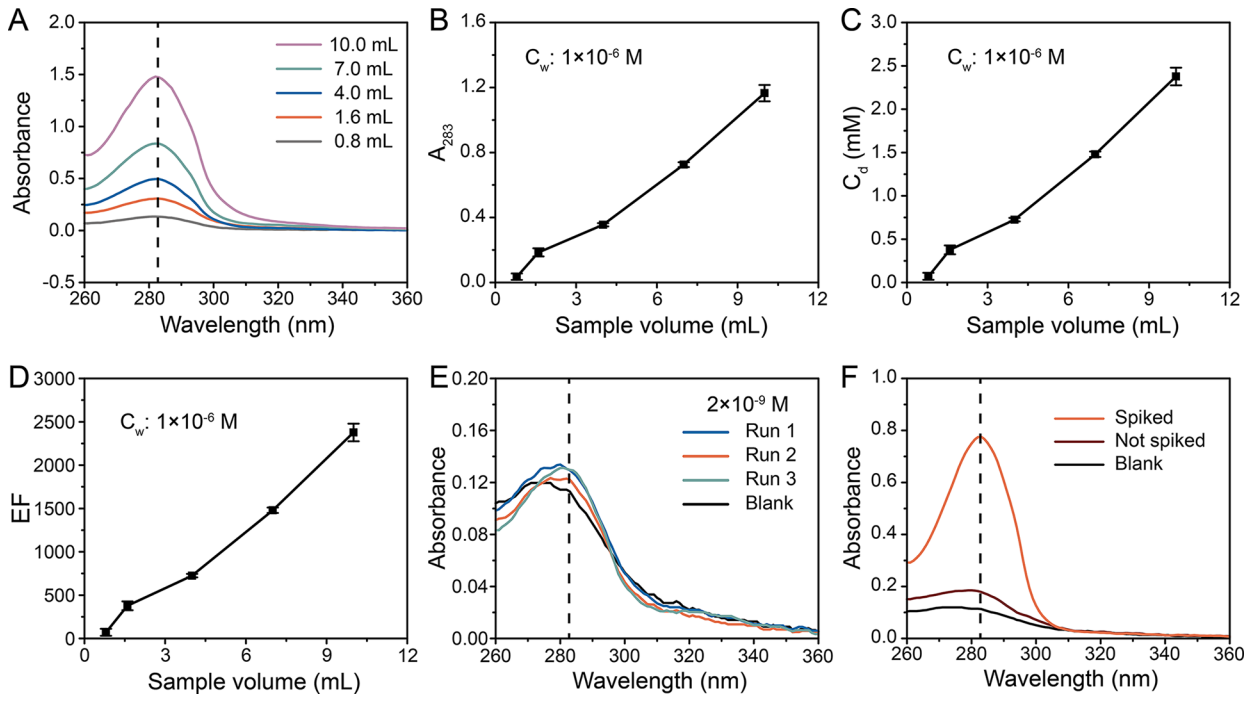

Figure 5. (A) UV−vis absorbance spectrum of collected octanol droplets. The droplets were from extractions with V from 0.8 to 10 mL/h. Q and C_w were 10 mL/h and 1 × 10^{-6} M. (B) A_{283} as a function of V. (C) C_d as a function of C_w. (D) EF as a function of C_w. (E) UV−vis spectrum of droplets extracting 100 mL sample with C_w of 2 × 10^{-9} M. (F) UV−vis spectrum of droplets extracting river water (North Saskatchewan River, Edmonton) spiked with 10^{-6} M triclosan. Q and V were 30 mL/h and 7 mL.

the solution A composition on the droplet size during solvent exchange.[38,39] As in Figure 5E, the LOD was found to be 2 × 10^{-9} M (~0.58 μg/L), which is comparable to previously published works listed in Table 1. As the concentration of the analyte was maintained constant, the maximum extractable amount of analyte is expected to increase with the increase of sample volume. However, the exact maximum extractable amount of analyte from the sample is hard to predict. We did not further increase the sample volume to improve the extraction performance, as a small enhancement consumes much more sample and extraction time. Additionally, the droplet dissolution from a higher sample volume makes it difficult to collect enough droplets or get reliable results.

Table 1. Comparison of the Proposed Method with Other Analytical Techniques[a]

analyte	extraction method	LOD (μg/L)	V (mL)	T (min)
triclosan	IL/IL-DLLME-HPLC-MS/MS[40]	0.23−0.35	5	2.5−12.5
triclosan	SSME-UV[41]	0.28	5	2−10
triclosan	DLLME-SFO[42]	0.1	5	1
triclosan	SLLME-UV (this work)	0.58	0.8−10	2−10
chlorpyrifos	WE-DLLME-GCFID[43]	0.92	10	5
chlorpyrifos	LLME-HPLC-UV[44]	0.1−0.35	10	4
chlorpyrifos	SLLME-UV (this work)	1.05	8	16

[a]V: sample volume; t: extraction time IL: ionic liquid; SSME: supramolecular microextraction; UV: ultraviolet; SFO: solidification of floating organic droplet; SLLME: surface nanodroplet-based liquid−liquid microextraction; WE: water emulsion; GCFID: gas chromatography flame ionization detector.

It is worth noting that the standard deviation of C_d and EF calculated from three replicates was found to be comparable to the average when C_d is low. The large deviation prevents the sensitive detection and precise quantification of samples at a lower concentration C_w. On the basis of results from standard solutions in Figure 3A,B, the measurement of the equipment did not account for the large deviation of A_{283}. Moreover, as the scale of deviation did not increase monotonically with C_w and C_d, the real concentration of triclosan in droplets C_d was not the only contributor of the deviation of A_{283}. The background also contributed to the large deviation of C_d and EF in results. An additional blank group with V = 10 mL was tested, showing A_{283} from the background is not relevant to V. The background peak at 283 nm was not from contaminants in the sample solution. Figure S1 compares the UV−vis spectrum from blank groups with V = 1.6 mL and V = 10 mL. A_{283} from the blank group can be applied for the correction of C_d in experiments with different V.

The droplet extraction was also performed with river water (North Saskatchewan River, Edmonton) spiked with 10^{-6} M triclosan. Q and V were kept at 30 mL/h and 7 mL. Figure 5F compares the UV−vis absorbance of collected octanol droplets from a spiked river sample, an unspiked river sample, and a blank water sample.

Performance of Chlorpyrifos Extraction. The organophosphate pesticide chlorpyrifos was taken as the second model compound for droplet extraction in the capillary.[45−47] The flow rate Q and sample volume V were 30 mL/h and 8 mL, respectively. The concentration of chlorpyrifos in samples C_w was from 10^{-6} to 2 × 10^{-8} M. Figure 6A shows the UV−vis spectra of collected nanodroplets, in which the peaks at 230 and 292 nm were identified as characteristic peaks of chlorpyrifos for quantitative analysis. As the background

https://doi.org/10.1021/acs.langmuir.2c01242
Langmuir 2022, 38, 11227−11235

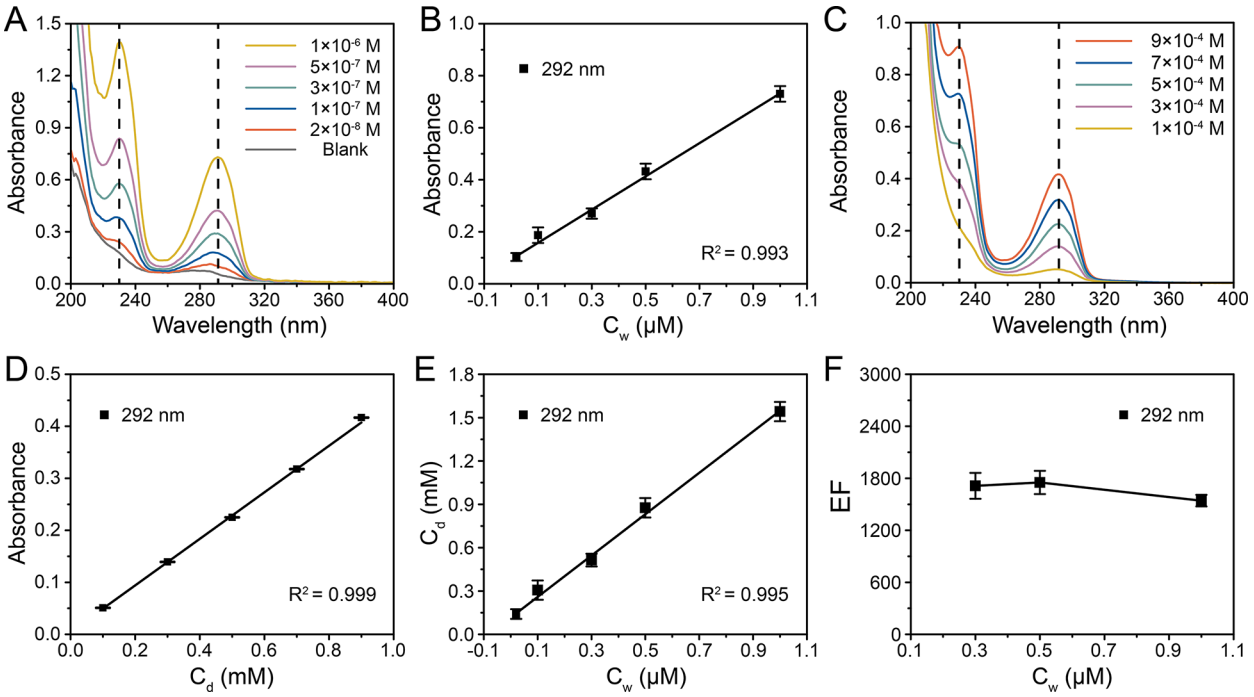

Figure 6. (A) UV−vis absorbance spectrum of collected octanol droplets. The concentrations of chlorpyrifos in samples were from 2×10^{-8} to 10^{-6} M. Q and V were 30 mL/h and 8 mL. (B) A_{292} as the functions of C_w. (C) UV−vis absorbance spectrum of chlorpyrifos in octanol standard solutions. The concentration of triclosan in the standard solutions is from 5×10^{-5} to 1.4×10^{-3} M. (D) A_{292} as the functions of C_d. (E) C_d as a function of C_w. (F) EF as a function of C_w.

signals at 230 nm was above 0.2, the quantitative analysis was only performed for the absorbance at 292 nm.

The absorbance at 292 nm (A_{292}) is plotted as a function of C_w in Figure 6B, which is found to increase monotonically with C_w. Similar to the results in Figure 2A, superposition of the absorbance from the background and chlorpyrifos at a low C_w leads to the highest absorbance moving to a lower wavelength. The highest absorbance shifted to 288 nm in the group of $C_w = 10^{-7}$ M and to 286 nm in the group of $C_w = 2 \times 10^{-7}$ M. Further reducing C_w may contribute to indistinguishable absorbance from the background and the analyte.

Figure 6C shows the UV−vis spectrum of chlorpyrifos in octanol standard solutions with C_d from 10^{-4} to 9×10^{-4} M. From the spectrum of standard solutions, A_{292} was plotted as a function of C_d in Figure 6D. From the Beer−Lambert law, C_d and EF were respectively calculated and plotted in Figure 6E,F. Similar to results in Figure 3D, the enrichment factor fluctuated in a small range from 1400 to 1900 at above 3×10^{-7} M. As the quantification of triclosan below 3×10^{-7} M may not be accurate, these data were not included in Figure 6F. The recovery of triclosan was estimated to be between 33 and 40%. The purpose of using chlorpyrifos is to confirm the quantitative analysis of our method was not limited by triclosan. The study of the influence of sample volume and sample flow rate can be repeated for chlorpyrifos or any other analytes of interest.

The extraction was performed with 80 mL samples to enhance the LOD of the method. The octanol volume ratio in solution A was increased to 4 vol %. Solution B was saturated with octanol before spiked with chlorpyrifos. As in Figure 7A, the LOD was enhanced to 3×10^{-9} M (~1.05 μg/L), which is comparable to previously published works listed in Table 1. The combinative extraction of triclosan and chlorpyrifos was performed by spiking solution B with two model compounds

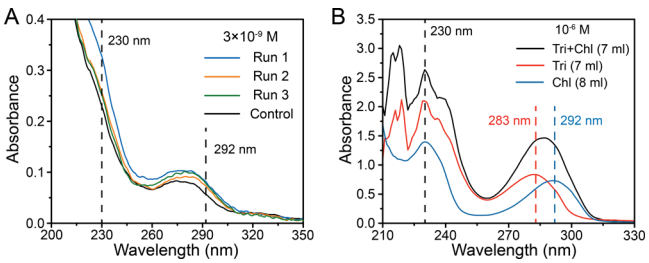

Figure 7. (A) UV−vis spectrum of droplets extracting 80 mL sample with chlorpyrifos of 3×10^{-9} M. (B) Comparing UV−vis spectra from the combinative extraction of triclosan and chlorpyrifos and single-component extraction.

both at a C_w of 10^{-6} M. The sample volume V and the volume flow rate Q were 7 and 30 mL/h. In Figure 7B, the UV−vis absorbance of the combinative extraction was compared with the spectra from single-component extraction. The combination of the characteristic peaks of triclosan at 283 nm and chlorpyrifos at 292 nm leads to a wide peak at 287 nm, demonstrating that multicomponents from the sample can be extracted at the same time.

GC-MS and Fluorescence Analysis of the Collected Drop. Nanoextraction by surface droplets can be applied in tandem with many common analytic tools for sensitive detection. The extraction of triclosan from water samples (7×10^{-6} M) was also confirmed by coupling with GC-MS. The peak appeared at 16.9 min in Figure 8A was identified to be triclosan.

As the final example, a fluorescent dye, Nile red was extracted from a pure water sample and a river water sample. C_w, Q, and V of the sample were 10^{-6} M, 30 mL/h, and 8 mL, respectively. After extraction, $a \geq 2$ μL octanol droplet was collected, as in Figure 8B,C. An optical microscope with

https://doi.org/10.1021/acs.langmuir.2c01242
Langmuir 2022, 38, 11227−11235

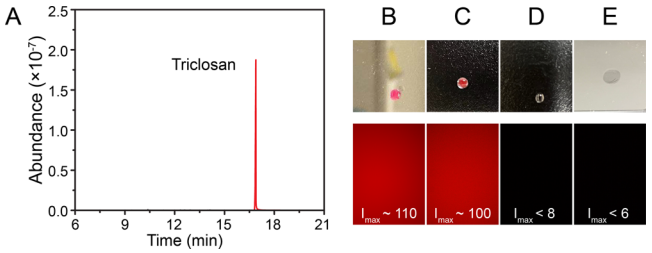

Figure 8. (A) GC results of the triclosan extracted by octanol droplets. (B–D) One drop (≥2 μL) of octanol collected from the extraction of (B) a pure water sample with the Nile red (10^{-6} M), (C) a river water sample with the Nile red (10^{-6} M), (D) a pure water sample without the Nile red, and their images from a fluorescence microscope. (E) One drop of pure water sample with the Nile red (10^{-6} M) and the image from a fluorescence microscope.

excitation lasers was used to test the fluorescent intensity of the droplet. As shown by the screenshot in Figure 8B,C, the maximum light intensity I_{max} of the drops were ∼110 and ∼100.

As a blank group, the same extraction process was performed for pure water (without Nile red). The fluorescence intensity of the collected octanol drop in the blank (Figure 8D) was less than 8. Therefore, the light intensity of ∼110 was mainly attributed to the extracted dye. Figure 8E show a drop of the pure water sample with a C_w of 10^{-6} M. The fluorescence intensity of the drop was less than 6. The extraction by surface droplets in the capillary tubes can also be used for the detection of fluorescent components in water samples.

The extractant is not limited to octanol for the surface nanodroplet-based extraction. The solvent exchange process can be used to produce a wide range of droplets based on the ouzo effect.[13] Surface nanodroplets consisting of other types of oils (oleic acid, EDGMEA) were also reported for extraction in previous work.[48]

CONCLUSION

In summary, we demonstrated a cost-saving extraction approach for concentrating and detecting trace amounts of chemical compounds using octanol surface nanodroplets formed inside a long capillary tube. The nanodroplets were produced by solvent exchange by using the sample solution as the second fluid. After extraction, nanodroplets could be collected by blowing a gentle stream of air. Because of the small volume and pinning effect, extraction based on surface nanodroplets in previous literature was limited to only a few online analytical techniques such as SERS and fluorescence microscope with limited model compounds. The collection of enough nanodroplets from a long capillary in this work enables offline analysis such as UV–vis and GC-MS.

The collected nanodroplets were analyzed by UV–vis spectrometry, which revealed a limit of detection of $\sim 10^{-9}$ M and a linear range above 2×10^{-7} M for two representative micropollutants, triclosan and chlorpyrifos, in water samples. Introducing the sample solution with a higher flow rate Q was found to speed up the process of droplet formation and extraction without compromising the extraction performance. Nanoextraction in the capillary was also confirmed to be compatible with other common analytical techniques including GC-MS and fluorescence microscopy. The method shown here is powerful for rapid extraction, quantification, and sensitive detection of a wide range of analytes in tandem with offline analytic instruments.

ASSOCIATED CONTENT

Supporting Information

The Supporting Information is available free of charge at https://pubs.acs.org/doi/10.1021/acs.langmuir.2c01242.

UV–vis absorbance of octanol from blank experiments (PDF)

AUTHOR INFORMATION

Corresponding Author

Xuehua Zhang − *Department of Chemical and Materials Engineering, University of Alberta, Alberta T6G 1H9, Canada; Physics of Fluids Group, Max Planck Center Twente for Complex Fluid Dynamics, JM Burgers Center for Fluid Dynamics, Mesa+, Department of Science and Technology, University of Twente, Enschede 7522 NB, The Netherlands;* orcid.org/0000-0001-6093-5324; Email: xuehua.zhang@ualberta.ca

Authors

Zhengxin Li − *Department of Chemical and Materials Engineering, University of Alberta, Alberta T6G 1H9, Canada;* orcid.org/0000-0003-0778-447X

Hongyan Wu − *Department of Chemical and Materials Engineering, University of Alberta, Alberta T6G 1H9, Canada*

Jae Bem You − *Department of Chemical and Materials Engineering, University of Alberta, Alberta T6G 1H9, Canada; Department of Chemical Engineering, Kyungpook National University, Daegu 41566, Republic of Korea;* orcid.org/0000-0003-0385-2295

Xiaomeng Wang − *Natural Resources Canada, CanmetENERGY Devon, Alberta T9G 1A8, Canada*

Hongbo Zeng − *Department of Chemical and Materials Engineering, University of Alberta, Alberta T6G 1H9, Canada;* orcid.org/0000-0002-1432-5979

Detlef Lohse − *Physics of Fluids Group, Max Planck Center Twente for Complex Fluid Dynamics, JM Burgers Center for Fluid Dynamics, Mesa+, Department of Science and Technology, University of Twente, Enschede 7522 NB, The Netherlands;* orcid.org/0000-0003-4138-2255

Complete contact information is available at: https://pubs.acs.org/10.1021/acs.langmuir.2c01242

Notes

The authors declare no competing financial interest.

ACKNOWLEDGMENTS

The authors acknowledge the funding support from Alberta Innovates, the Natural Science and Engineering Research Council of Canada (NSERC) Alliance Grant, the ERC Proof-of-Concept grant (Project No. 862032), Future Energy Systems (Canada First Research Excellence Fund), the start-up fund from Faculty of Engineering, University of Alberta, the Canada Research Chairs program, and the Canada Foundation for Innovation and Alberta Innovates.

REFERENCES

(1) Ingle, N.; Sayyad, P.; Deshmukh, M.; Bodkhe, G.; Mahadik, M.; Al-Gahouari, T.; Shirsat, S.; Shirsat, M. D. A chemiresistive gas sensor

for sensitive detection of SO2 employing Ni-MOF modified−OH-SWNTs and−OH-MWNTs. *Appl. Phys. A: Mater. Sci. Process.* **2021**, *127*, 1−10.
(2) Chaikhan, P.; Udnan, Y.; Ampiah-Bonney, R. J.; Chaiyasith, W. C. Air-assisted solvent terminated dispersive liquid−liquid microextraction (AA-ST-DLLME) for the determination of lead in water and beverage samples by graphite furnace atomic absorption spectrometry. *Microchemical Journal* **2021**, *162*, 105828.
(3) Lê, Q. T.; Ly, N. H.; Kim, M.-K.; Lim, S. H.; Son, S. J.; Zoh, K.-D.; Joo, S.-W. Nanostructured Raman substrates for the sensitive detection of submicrometer-sized plastic pollutants in water. *J. Hazard. Mater.* **2021**, *402*, 123499.
(4) Malby, A. R.; Whyatt, J. D.; Timmis, R. J. Conditional extraction of air-pollutant source signals from air-quality monitoring. *Atmos. Environ.* **2013**, *74*, 112−122.
(5) Mao, K.; Yang, Z.; Zhang, H.; Li, X.; Cooper, J. M. Wastewater-based nanosensors to evaluate community-wide illicit drug use for wastewater-based epidemiology. *Water Res.* **2021**, *189*, 116559.
(6) Hansen, F.; Oiestad, E. L.; Pedersen-Bjergaard, S. Bioanalysis of pharmaceuticals using liquid-phase microextraction combined with liquid chromatography−mass spectrometry. *J. Pharm. Biomed. Anal.* **2020**, *189*, 113446.
(7) Wang, K.; Zhang, R.; Yue, X.; Zhou, Z.; Bai, L.; Tong, Y.; Wang, B.; Gu, D.; Wang, S.; Qiao, Y.; et al. Synthesis of diboronic acid-based fluorescent probes for the sensitive detection of glucose in aqueous media and biological matrices. *ACS Sens.* **2021**, *6*, 1543−1551.
(8) Pal, S.; Ghosh, T. K.; Ghosh, R.; Mondal, S.; Ghosh, P. Recent advances in recognition, sensing and extraction of phosphates: 2015 onwards. *Coord. Chem. Rev.* **2020**, *405*, 213128.
(9) Zhang, Y.; Zhang, X.; Jiao, B. Determination of ten pyrethroids in various fruit juices: Comparison of dispersive liquid−liquid microextraction sample preparation and QuEChERS method combined with dispersive liquid−liquid microextraction. *Food Chem.* **2014**, *159*, 367−373.
(10) Huang, L.; Sun, D.-W.; Pu, H.; Wei, Q. Development of nanozymes for food quality and safety detection: Principles and recent applications. *Comprehensive Reviews in Food Science and Food Safety* **2019**, *18*, 1496−1513.
(11) Szarka, A.; Búčiková, K.; Kostić, I.; Hrouzková, S. Development of a multiresidue QuEChERS−DLLME—fast GC−MS method for determination of selected pesticides in yogurt samples. *Food Analytical Methods* **2020**, *13*, 1829−1841.
(12) Yamini, Y.; Rezazadeh, M.; Seidi, S. Liquid-phase microextraction - The different principles and configurations. *Trends in Analytical Chemistry* **2019**, *112*, 264−272.
(13) Lohse, D.; Zhang, X.; et al. Surface nanobubbles and nanodroplets. *Rev. Mod. Phys.* **2015**, *87*, 981.
(14) Lohse, D.; Zhang, X. Physicochemical hydrodynamics of droplets out of equilibrium. *Nature Reviews Physics* **2020**, *2*, 426−443.
(15) Jeannot, M. A.; Cantwell, F. F. Solvent microextraction into a single drop. *Anal. Chem.* **1996**, *68*, 2236−2240.
(16) He, Y.; Lee, H. K. Liquid-phase microextraction in a single drop of organic solvent by using a conventional microsyringe. *Anal. Chem.* **1997**, *69*, 4634−4640.
(17) Rasmussen, K. E.; Pedersen-Bjergaard, S. Developments in hollow fibre-based liquid-phase microextraction. *Trends in Analytical Chemistry* **2004**, *23*, 1−10.
(18) Rezaee, M.; Assadi, Y.; Hosseini, M.-R. M.; Aghaee, E.; Ahmadi, F.; Berijani, S. Determination of organic compounds in water using dispersive liquid−liquid microextraction. *Journal of Chromatography A* **2006**, *1116*, 1−9.
(19) Leong, M.-I.; Fuh, M.-R.; Huang, S.-D. Beyond dispersive liquid−liquid microextraction. *Journal of Chromatography a* **2014**, *1335*, 2−14.
(20) Almeida, C.; Fernandes, J.; Cunha, S. A novel dispersive liquid−liquid microextraction (DLLME) gas chromatography-mass spectrometry (GC−MS) method for the determination of eighteen biogenic amines in beer. *Food Control* **2012**, *25*, 380−388.
(21) Khodadoust, S.; Hadjmohammadi, M. Determination of N-methylcarbamate insecticides in water samples using dispersive liquid−liquid microextraction and HPLC with the aid of experimental design and desirability function. *Anal. Chim. Acta* **2011**, *699*, 113−119.
(22) Jovanov, P.; Guzsvány, V.; Franko, M.; Lazić, S.; Sakač, M.; Milovanović, I.; Nedeljković, N. Development of multiresidue DLLME and QuEChERS based LC−MS/MS method for determination of selected neonicotinoid insecticides in honey liqueur. *Food Research International* **2014**, *55*, 11−19.
(23) Gong, A.; Zhu, X. Miniaturized ionic liquid dispersive liquid−liquid microextraction in a coupled-syringe system combined with UV for extraction and determination of danazol in danazol capsule and mice serum. *Spectrochimica Acta Part A: Molecular and Biomolecular Spectroscopy* **2016**, *159*, 163−168.
(24) Tobiszewski, M.; Mechlińska, A.; Namieśnik, J. Green analytical chemistry—theory and practice. *Chem. Soc. Rev.* **2010**, *39*, 2869−2878.
(25) Tobiszewski, M. Metrics for green analytical chemistry. *Analytical Methods* **2016**, *8*, 2993−2999.
(26) Zhang, X.; Lu, Z.; Tan, H.; Bao, L.; He, Y.; Sun, C.; Lohse, D. Formation of surface nanodroplets under controlled flow conditions. *Proc. Natl. Acad. Sci. U. S. A.* **2015**, *112*, 9253−9257.
(27) Li, Z.; Kiyama, A.; Zeng, H.; Lohse, D.; Zhang, X. Speeding up biphasic reactions with surface nanodroplets. *Lab Chip* **2020**, *20*, 2965−2974.
(28) Wei, Z.; You, J. B.; Zeng, H.; Zhang, X. Interfacial partitioning enhances microextraction by multicomponent nanodroplets. *J. Phys. Chem. C* **2022**, *126*, 1326−1336.
(29) Li, M.; Dyett, B.; Zhang, X. Automated femtoliter droplet-based determination of oil−water partition coefficient. *Anal. Chem.* **2019**, *91*, 10371−10375.
(30) Dyett, B.; Zhang, Q.; Xu, Q.; Wang, X.; Zhang, X. Extraordinary focusing effect of surface nanodroplets in total internal reflection mode. *ACS Central Science* **2018**, *4*, 1511−1519.
(31) Li, M.; Dyett, B.; Yu, H.; Bansal, V.; Zhang, X. Functional femtoliter droplets for ultrafast nanoextraction and supersensitive online microanalysis. *Small* **2019**, *15*, 1804683.
(32) Wei, Z.; Li, M.; Zeng, H.; Zhang, X. Integrated nanoextraction and colorimetric reactions in surface nanodroplets for combinative analysis. *Anal. Chem.* **2020**, *92*, 12442−12450.
(33) You, J. B.; Lohse, D.; Zhang, X. Surface nanodroplet-based nanoextraction from sub-milliliter volumes of dense suspensions. *Lab Chip* **2021**, *21*, 2574−2585.
(34) Tohidi, F.; Cai, Z. GC/MS analysis of triclosan and its degradation by-products in wastewater and sludge samples from different treatments. *Environ. Sci. Pollut. Res.* **2015**, *22*, 11387−11400.
(35) Quan, B.; Li, X.; Zhang, H.; Zhang, C.; Ming, Y.; Huang, Y.; Xi, Y.; Weihua, X.; Yunguo, L.; Tang, Y. Technology and principle of removing triclosan from aqueous media: A review. *Chem. Eng. J.* **2019**, *378*, 122185.
(36) Levy, C. W.; Roujeinikova, A.; Sedelnikova, S.; Baker, P. J.; Stuitje, A. R.; Slabas, A. R.; Rice, D. W.; Rafferty, J. B. Molecular basis of triclosan activity. *Nature* **1999**, *398*, 383−384.
(37) Liu, K.; Chen, L.; Huang, L.; Ni, Y.; Sun, B. Enhancing antibacterium and strength of cellulosic paper by coating triclosan-loaded nanofibrillated cellulose (NFC). *Carbohydr. Polym.* **2015**, *117*, 996−1001.
(38) Lu, Z.; Xu, H.; Zeng, H.; Zhang, X. Solvent effects on the formation of surface nanodroplets by solvent exchange. *Langmuir* **2015**, *31*, 12120−12125.
(39) Lu, Z.; Peng, S.; Zhang, X. Influence of solution composition on the formation of surface nanodroplets by solvent exchange. *Langmuir* **2016**, *32*, 1700−1706.
(40) Zhao, R.-S.; Wang, X.; Sun, J.; Hu, C.; Wang, X.-K. Determination of triclosan and triclocarban in environmental water samples with ionic liquid/ionic liquid dispersive liquid-liquid microextraction prior to HPLC-ESI-MS/MS. *Microchimica Acta* **2011**, *174*, 145−151.

https://doi.org/10.1021/acs.langmuir.2c01242
Langmuir 2022, 38, 11227−11235

(41) Mpupa, A.; Mashile, G. P.; Nomngongo, P. N. Vortex assisted-supramolecular solvent based microextraction coupled with spectrophotometric determination of triclosan in environmental water samples. *Open Chemistry* **2017**, *15*, 255−262.
(42) Zheng, C.; Zhao, J.; Bao, P.; Gao, J.; He, J. Dispersive liquid−liquid microextraction based on solidification of floating organic droplet followed by high-performance liquid chromatography with ultraviolet detection and liquid chromatography−tandem mass spectrometry for the determination of triclosan and 2, 4-dichlorophenol in water samples. *Journal of Chromatography A* **2011**, *1218*, 3830−3836.
(43) Farajzadeh, M. A.; Mogaddam, M. R. A.; Esrafili, L. Surfactant-less water emulsion based dispersive liquid−liquid microextraction for determination of organophosphorus pesticides in aqueous samples. *Analytical Methods* **2015**, *7*, 7899−7906.
(44) Zohrabi, P.; Shamsipur, M.; Hashemi, M.; Hashemi, B. Liquid-phase microextraction of organophosphorus pesticides using supramolecular solvent as a carrier for ferrofluid. *Talanta* **2016**, *160*, 340−346.
(45) Fleeger, J. W.; Carman, K. R.; Nisbet, R. M. Indirect effects of contaminants in aquatic ecosystems. *Sci. Total Environ.* **2003**, *317*, 207−233.
(46) Singh, B. K.; Walker, A. Microbial degradation of organophosphorus compounds. *FEMS Microbiology Reviews* **2006**, *30*, 428−471.
(47) Solomon, K. R.; Williams, W. M.; Mackay, D.; Purdy, J.; Giddings, J. M.; Giesy, J. P. Properties and uses of chlorpyrifos in the United States. *Ecological Risk Assessment for Chlorpyrifos in Terrestrial and Aquatic Systems in the United States* **2014**, *231*, 13−34.
(48) Li, M.; Cao, R.; Dyett, B.; Zhang, X. Encapsulated Nanodroplets for Enhanced Fluorescence Detection by Nano-Extraction. *Small* **2020**, *16*, 2004162.

https://doi.org/10.1021/acs.langmuir.2c01242
Langmuir 2022, 38, 11227−11235